

Numerical Analysis of the Drag Coefficient on Energy-Efficient Vehicle Prototypes

Hendry Sakke Tira^{a,*}, Muhammad Agus Muliawan^a, Syahrul^a

^a Department of Mechanical Engineering, Faculty of Engineering, University of Mataram
Jalan Majapahit No 62, Mataram 83115 Nusa Tenggara Barat Indonesia

*hendrytira@unram.ac.id

Abstract

The focus of this investigation is to determine the drag coefficient on the prototype vehicle and also the pressure profile on the entire body of the prototype. The study was carried out on a prototype vehicle that would compete at Shell Eco-Marathon Asia-Pacific and Middle East 2023. The test was performed on an energy-efficient vehicle prototype built by the Mandalika Desantara Team, a team of mechanical engineering students at Mataram University. To accomplish this, a CFD approach simulation was performed using the Ansys 2023 R2 simulation software - fluent flow with a comparison of the drag coefficient and average pressure and wind speed of 30 km/h. According to the simulation results, the average drag coefficient value on the prototype design is 0.194. The highest average pressure can be detected on the front of the vehicle, where that part has a maximum pressure of 101374 Pa. While the airflow over the prototype body has the highest average speed of around 10 m/s. Based on these results, the prototype vehicle design still needs to be improved in order to compete in similar competitions.

Keywords: drag coefficient, prototype vehicle, Mandalika Team, Shell Eco-Marathon

Abstrak

Penelitian ini bertujuan untuk mengetahui koefisien drag pada prototipe kendaraan dan untuk mengetahui profil tekanan pada sekujur body dari prototipe tersebut. Penelitian dilakukan pada sebuah kendaraan prototipe yang akan dilombakan pada sebuah event. Adapun pengujian dilakukan pada kendaraan prototipe efisien energi dari Tim Mandalika Desantara jurusan teknik mesin Universitas Mataram. Untuk mencapai hal tersebut dilakukan simulasi pendekatan CFD dengan menggunakan software simulasi Ansys 2023 R2 - flow fasih dengan perbandingan koefisien drag dan tekanan rata-rata serta kecepatan angin yaitu 30 km/jam. Hasil simulasi diperoleh nilai koefisien drag rata-rata pada desain prototype adalah 0,194. Melalui simulasi ini, rata-rata diperoleh tekanan tertinggi terdapat pada bodi depan kendaraan, dimana bagian tersebut memiliki tekanan maksimal sebesar 101374 Pa. Sedangkan kecepatan rata-rata tertinggi terdapat pada aliran udara di atas bodi prototipe sekitar 10 m/s. Atas hasil tersebut maka desain kendaraan prototipe masih memerlukan perbaikan untuk dapat bersaing dalam kompetisi sejenis.

Kata kunci: koefisien hambat, kendaraan prototipe, Tim Mandalika, Shell Eco-Marathon

1. Introduction

The growing number of vehicles has had a significant impact on fuel consumption and environmental degradation over time. This rise contributes to the depletion of non-renewable fuel reserves and worsens the emission of exhaust gases that harm the environment [1-2]. Continuous mitigation efforts are being made to minimize fuel consumption, including through the design of energy-efficient vehicles. Various competitions for energy-efficient vehicles are organized to encourage participants from different countries to apply their knowledge and creativity in building and designing efficient vehicles. One prominent example is the Shell Eco-Marathon Asia-Pacific and Middle East 2023, an international competition focused on energy-efficient vehicles, which serves as a platform for industry stakeholders to collaborate. It is not only companies that participate, but also universities from Indonesia and the Asia-Pacific region, including University of Mataram. The achievements of Universitas Mataram in the competition held in July 2023 at the international Mandalika circuit in West Nusa Tenggara Province, Indonesia, reflect its ability to send an energy-efficient vehicle prototype that successfully advanced to the final stage.

To achieve energy efficiency, several strategies can be adopted. Modifying the propulsion system, selecting lightweight materials in vehicle design, and optimizing aerodynamic factors are some approaches that can be pursued [3-4]. Aerodynamic factors play a crucial role in designing efficient vehicles. The close relationship between the shape of the vehicle body and its interaction with external factors, such as airflow, is a key element in minimizing the resistance faced by the vehicle [5]. Optimal aerodynamics not only impact increasing the vehicle's speed but also reducing fuel consumption. This is due to the minimized resistance, enabling the vehicle to move with lower power. Lower power consumption during vehicle movement results in significant fuel savings [6].

Among the vehicle components, the front and roof of the car play a significant role in shaping aerodynamic drag. In this context, improving aerodynamic efficiency can lead to substantial fuel savings. A previous study stated that an increase in vehicle aerodynamics can contribute to a decrease in fuel consumption by 3-4% and a decrease in drag force by 10%. [7]. The drag force phenomenon is critical as it hampers the vehicle's movement. This force highly depends on dimensions, body shape, and vehicle speed. Thus, careful and precise vehicle body design planning is a key strategy in reducing this drag force [8].

The energy-efficient vehicle prototype submitted by University of Mataram for the Shell Eco-Marathon competition has been meticulously adapted to comply with the regulations in place. The dimensions and shape of the vehicle body have been carefully considered to reduce the resistance encountered during the journey. The selection of materials and body thickness is also a crucial consideration in creating a lightweight yet rigid body. In measuring the resistance faced by the designed vehicle, the Computational Fluid Dynamics (CFD) method is a rational choice. This method not only provides accurate results but is also cost-effective through the use of specialized software [9]. This approach has been consistently employed in related research to measure the drag force on planned energy-efficient vehicles. Therefore, the goal of this research corresponds with the previously laid out objectives, aiming to measure the drag force values encountered by energy-efficient vehicle prototypes. Given the unique geometry and shape of each vehicle prototype, this research is expected to provide reference values on drag force that are useful in the design and production of future energy-efficient vehicles.

2. Materials and methods

In order to achieve the goal of this research, which is to obtain the smallest possible drag value for the energy-efficient prototype vehicle, the front part of the prototype car is designed to be streamlined (Figure 1). With this shape, it is anticipated that air can easily pass through the vehicle's body, resulting in a lower coefficient of drag.

The development of prototype body geometry using Fusion 360 has served as a pivotal initial step in the design process of the vehicle for the Shell Eco-Marathon Asia Pacific and Middle East 2023 competition. Subsequently, the focus shifted towards critical simulations employing Computational Fluid Dynamics (CFD) through the Ansys 2023 R2 software. The fluid flow simulation feature within Ansys 2023 R2 plays a central role in assisting experts and engineers in the broader development and design process of objects, a role especially pertinent to this research.

The significance of this fluid flow simulation feature becomes more pronounced due to the intricate design complexities of the prototype body, meticulously aligned with the guidelines and parameters of the Shell Eco-Marathon 2023 competition. The dimensions of the prototype vehicle are presented in table 1.

Table 1. Prototype vehicle dimensions

| Dimension | Data (mm) |
|-----------|-----------|
| Length | 3277.277 |
| Width | 994.912 |
| Height | 625.516 |

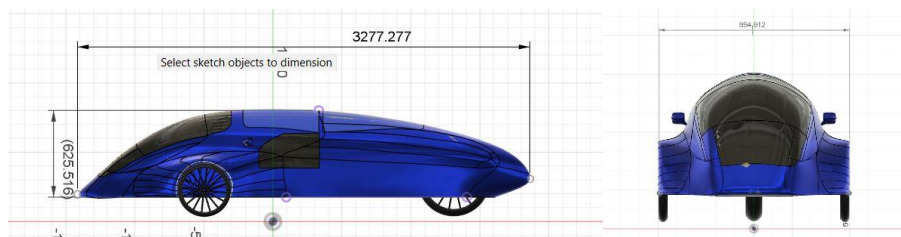


Figure 1. Vehicle design and dimensions

Simulation steps

The first stage of the simulation and data analysis is to establish and integrate boundaries. The distance between the boundary and the car body is adjusted during the boundary-making process to ensure that it is not excessively far or excessively close, with the assumption that this boundary is a tunnel. The size of the boundary is shown in the table 2.

Table 2. Boundary dimensions

| Parameters | Distance from the body to the boundary (mm) |
|------------|---|
| Top | 100 |
| Bottom | 1 |
| Left side | 1000 |
| Right side | 1000 |
| Frontage | 1000 |

| | |
|------|------|
| Rear | 1000 |
|------|------|

The next step is to mesh the prototype body, which has been given the boundary parameters shown in table 3 below.

Table 3. Meshing data

| Parameters | Data |
|--------------------|---------|
| Element size | 778 mm |
| Maximum size | 1000 mm |
| Number of nodes | 166072 |
| Number of elements | 924644 |
| Skewness quality | 0.23771 |
| Orthogonal quality | 0.76102 |

The next step is to put in the parameters over the boundary conditions or environmental conditions at the boundary, as well as the wind flow speed that is closest to the actual conditions in the location, as shown in table 4.

Table 4. Ambient parameters

| Parameters | Data |
|---------------------|-------------------------|
| Ambient temperature | 24°C |
| Ambient pressure | 101325 Pa |
| Wind speed | 30 km/h |
| Air density | 1.225 kg/m ³ |

To get results that are in line with the outcome desired, the direction of the airflow and the variable to be examined must be determined. Since the vehicle is assumed to move forward, the air in this simulation originates from the front side. The drag coefficient value of the prototype vehicle is the variable to be sought. In order to get more accurate results, the calculation is performed 1000 times. However, the more iterations there are, the longer the calculation process will take. This will have an effect on the computer that will be used for the simulation.

3. Results and discussion

3.1 Drag coefficient

After the calculation process is complete, the output result is in the form of a drag coefficient with a value of $C_d = 0.194$ at a speed of 30 km/h.

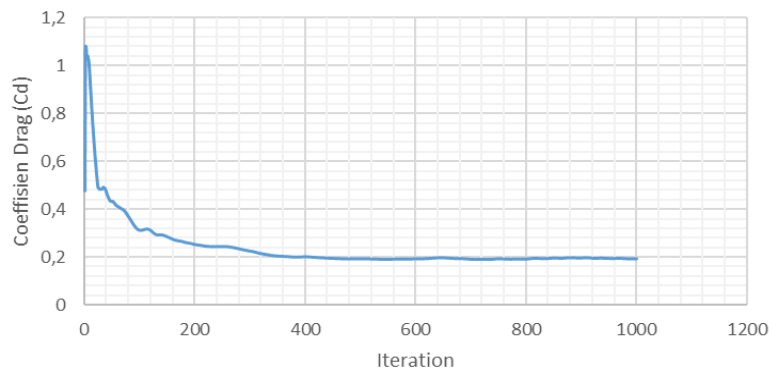


Figure 2. Coefficient of drag value

The results of the drag coefficient on the simulated energy-efficient prototype vehicle are shown in Figure 2. This value is quite high for a prototype type vehicle, where the prototype vehicle is a vehicle with an aerodynamic design model. This prototype vehicle has a higher drag coefficient value than the Jayabaya 1.0 prototype vehicle, which has a drag coefficient value of $C_d = 0.142$ at the same speed. The Jayabaya 1.0 prototype vehicle's C_d value is 26.8% lower than the simulated prototype vehicle's C_d value [10].

The elevated coefficient of drag (C_d) value observed in the simulated energy-efficient prototype vehicle poses a challenge that necessitates deeper analysis. C_d is a measure of how much an object encounters resistance to the fluid flow when in motion. A higher C_d value indicates that the vehicle encounters more air resistance, which in turn can diminish energy efficiency and overall performance [11]. The increase in C_d value in this prototype vehicle, particularly when compared to the lower C_d value on other prototype vehicle, can be attributed to several factors such as suboptimal geometric design. An aerodynamically suboptimal body design can lead to turbulence and zones of resistance in the airflow around the vehicle. This might result from geometric complexities or insufficient attention to aerodynamic

aspects during the design process. Another factor is surface imperfections. An uneven vehicle surface or specific imperfections can influence the airflow around the vehicle, leading to heightened turbulence and increased resistance [12-13].

Furthermore, incompatibility with Simulation Speed can be another reason. Cd values can significantly change with variations in the speed of the airflow. It's plausible that this vehicle's design is better suited for a different speed than what was simulated, influencing the resultant Cd value [14-15]. CFD simulation outcomes can also be affected by numerical factors such as grid size, solution methods, and boundary conditions applied within the simulation. These factors can impact the final simulation results. In order to address these concerns, further investigation and analysis are crucial. By comprehensively understanding these contributing factors, designers can work towards optimizing the vehicle's aerodynamics, ultimately aiming to reduce the drag coefficient and enhance overall efficiency and performance.

3.2 Pressure Resistance

According to the simulation results, the highest pressure point is at the front end of the vehicle, with a pressure value of 101374 Pa at a speed of 30 km/h. This pressure is 49 Pa higher than normal air pressure, which is 101325 Pa. Figure 3 shows that the front area has higher pressure than the rest of the area. Based on the area, the front obstacle area is still too large, so changes must be made to reduce the obstacle area.

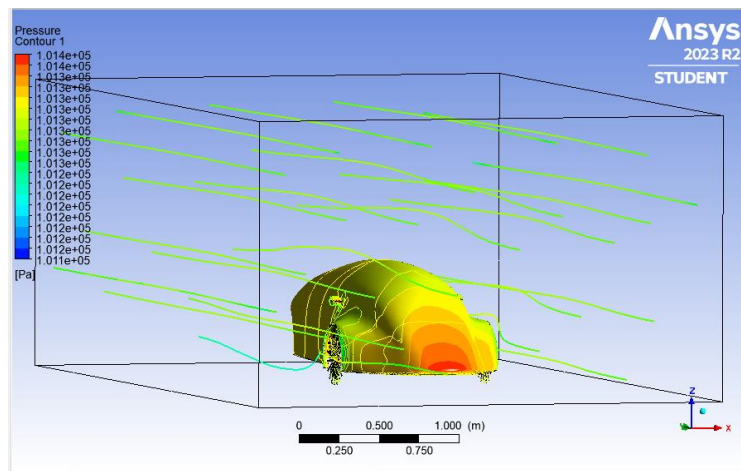


Figure 3. Contour of surface on surface

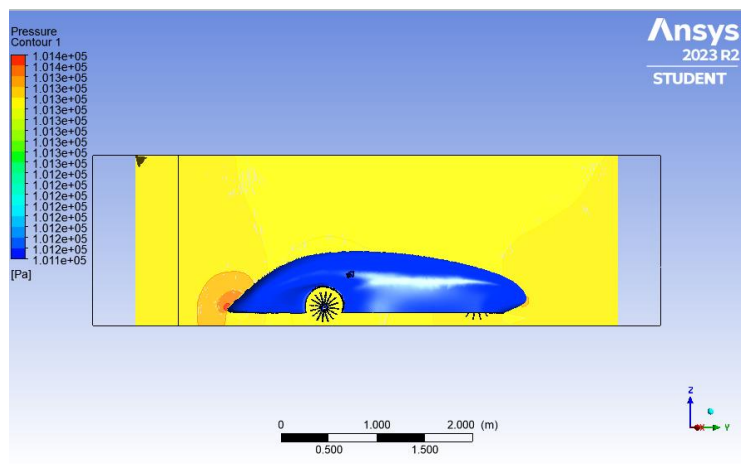


Figure 4. Contour of pressure at boundary

The pressure in the area around the vehicle is depicted in Figure 4. At a speed of 30 km/h, the orange front area has the highest pressure. The yellow color on the vehicle's front and rear is darker. Meanwhile, the vehicle's top is a brighter yellow color. This means that the air pressure at the vehicle's front and rear is greater than the air pressure at the vehicle's top.

The pressure increase can lead to significant aerodynamic resistance, as the high pressure at the front part creates a drag force that impedes the vehicle's movement. As the vehicle moves, the airflow flows around its surface. When the airflow encounters the front surface of the vehicle, several phenomena occur, such as the formation of a stagnation zone [16]. At the initial point of contact between the airflow and the vehicle's surface, the airflow slows down and even

momentarily stops. This is known as the stagnation zone. At this point, the air pressure increases due to the conversion of the airflow's kinetic energy into potential pressure energy [17].

Another phenomenon is the diversion of airflow. The flowing air that moves around the vehicle gets redirected. At the front of the vehicle, the airflow must 'bend' and maneuver around the vehicle. This results in a higher-pressure zone in front of the vehicle [18]. The solution to reduce this resistance is by designing a more aerodynamic vehicle body. By streamlining or redirecting the airflow more effectively around the vehicle, the stagnation zones and high pressure at the front can be better managed. This, in turn, decreases drag forces and enhances overall efficiency.

3.3 Velocity contour

The simulation results of the airflow velocity contour in Figure 5 show that the airflow velocity is lower in areas of higher pressure. The lower the airflow velocity, the higher the pressure at that point, and vice versa. According to the figure, the highest airspeed is located above the vehicle body, with a value of around 11.73 m/s, and the lowest airspeed is behind the prototype vehicle, with a value of around 2.347 m/s.

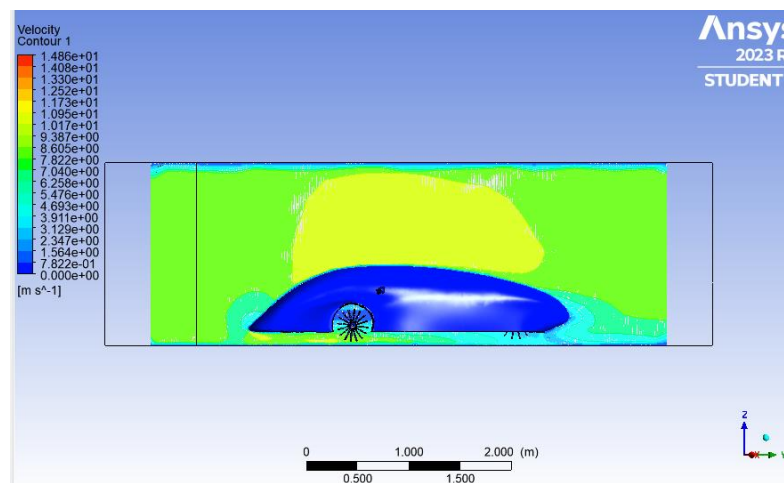


Figure 5. Contour of velocity at boundary

This phenomenon arises due to the presence of the Bernoulli principle. The Bernoulli principle states that in a fluid flow devoid of significant mechanical work, an increase in flow velocity leads to a decrease in pressure, and conversely, an increase in pressure results in a reduction in flow velocity [19]. This principle illustrates the relationship between kinetic energy and potential energy within fluid flow. In vehicle sections where pressure increases occur, the airflow is compelled to decelerate. This is due to the fact that the kinetic energy of the airflow diminishes as potential pressure energy rises, consequently causing a reduction in flow velocity. This phenomenon illustrates how the airflow adapts to the contour of the vehicle's surface, generating distinct pressure and velocity patterns around the vehicle.

4. Summary

According to the findings of the analysis, the drag coefficient is $C_d = 0.194$. This value seems quite large when compared to the drag coefficient values on other prototype vehicles at the same airspeed of 30 km/h. The highest resistance pressure of 101374 Pa is found at the front of the prototype vehicle body. The pressure rises by 49 Pa from atmospheric pressure. Furthermore, the highest speed on the speed contour scale is approximately 11.73 m/s, which occurs in the area above the prototype vehicle body, and the lowest speed is approximately 2.347 m/s, which occurs in the rear area. Based on the simulation results, the shape of this prototype vehicle needs to be improved in order to reduce drag and improve aerodynamics.

5. Acknowledgement

The author would like to thank those who contributed to making this article possible and supported the Mandalika Desantara team of mechanical engineering department compete in the Shell Eco-Marathon Asia-Pacific and Middle East 2023 competition, namely the Faculty of Engineering and Mataram University.

References

- [1] Tira, H. S., Zulfikar, M. P., Sayoga, I. M. A., 2023, "Numerical Study of Flat-top Piston Head Structure Under Different Materials" *Rotasi*, 25: 1–6.
- [2] Yao, Z., Wang, Y., Liu, B., Zhao, B., Jiang, Y., 2021, "Fuel consumption and transportation emissions evaluation of mixed traffic flow with connected automated vehicles and human-driven vehicles on expressway" *Energy*, 230: 120766.
- [3] Li, Q. Q., Li, E., Chen, T., Wu, L., Wang, G. Q., He, Z. C., 2021, "Improve the frontal crashworthiness of

- vehicle through the design of front rail" *Thin-Walled Structures*, 162: 107588.
- [4] Zhang, Y., Xu, S., Wan, Y., 2020, "Performance improvement of centrifugal compressors for fuel cell vehicles using the aerodynamic optimization and data mining methods" *Int. J. Hydrogen Energy*, 45: 11276-11286.
- [5] Mukut, A. N. M. M. I., Abedin, M. Z., 2019, "Review on Aerodynamic Drag Reduction of Vehicles" *International Journal of Engineering Materials and Manufacture*, 4: 1–14.
- [6] Brandt, A., Jacobson, B., Sebben, S., 2022, "High speed driving stability of road vehicles under crosswinds : an aerodynamic and vehicle dynamic parametric sensitivity analysis sensitivity analysis" *Vehicle System Dynamics*, 60: 2334-2357.
- [7] Ambo, K., Nagaoka, H., 2020, "Aerodynamic force prediction of the laminar to turbulent flow transition around the front bumper of the vehicle using Dynamic-slip wall model LES" *American Institute of Aeronautics and Astronautics SciTech Forum*, 1–18.
- [8] Czyż, Z., Karpiński, P., Koçak, S., 2019, "Numerical Analysis of the Influence of Particular Parts of the High Efficient Electric Vehicle on the Aerodynamic Forces" *Advances in Science and Technology Research Journal*, 13: 1–7.
- [9] Duan, X., Liu, Y., Liu, J., Lai, M., Jansons, M., Guo, G., Zhang, S., Tang, Q., 2019, "Experimental and numerical investigation of the effects of low-pressure , high-pressure and internal EGR configurations on the performance , combustion and emission characteristics in a hydrogen-enriched heavy-duty lean-burn natural gas SI engine" *Energy Convers. Manag.*, 195: 1319–1333.
- [10] Ananda, R. P., Pramesti, Y. S., Akbar, A., 2021, "Analisis Aerodinamika Bodi Kendaraan KMHE Jayabaya Prototype 2.0" *Seminar Nasional Inovasi Teknologi*, 218-223.
- [11] Jaffar, F., Farid, T., Sajid, M., Ayaz, Y., Khan, M. J., 2020 "Prediction of Drag Force on Vehicles in a Platoon Configuration Using Machine Learning" *IEEE Access*, 8: 201823–201834.
- [12] Donald, M., Bolzon, P., Sebben, S., Broniewicz, A., 2019 "Effects of wheel configuration on the flow field and the drag coefficient of a passenger vehicle" *Int. J. Automotive Technology*, 20: 763–777.
- [13] Urquhart, M., Varney, M., Sebben, S., Passmore, M., 2020 "Aerodynamic drag improvements on a square-back vehicle at yaw using a tapered cavity and asymmetric flaps" *Int. J. Heat Fluid Flow*, 86: 108737.
- [14] Nath, D, S., Pujari, P, C., Jain, A., Rastogi, V., 2021 "Drag reduction by application of aerodynamic devices in a race car" *Advances in Aerodynamics*, 3" 1-20.
- [15] Ganesan, S., Esakki B., 2020 "Computational fluid dynamic analysis of an unmanned amphibious aerial vehicle for drag reduction" *Int. J. Unmanned systems*, 8: 187–200.
- [16] Kaluva, S, T., Pathak, A., Ongel, A., 2020 "Aerodynamic Drag Analysis of Autonomous Electric Vehicle Platoons" *Energies*, 13: 4028.
- [17] Tarakka, R., Salam, N., Jalaluddin, Ihsan, M., 2019 "Effect of Blowing Flow Control and Front Geometry Towards the Reduction of Aerodynamic Drag on Vehicle Models" *FME Transactions*, 47: 552–559.
- [18] Maji, B, S, B., Mustafa, N., 2022, "CFD Analysis of Rear-Spoilers Effectiveness on Sedan Vehicle in Compliance with Malaysia National Speed Limit" *Journal of Automotive Powertrain and Transportation Technology*, 1: 26–36.
- [19] Chawla, R., Pakrashi V., 2022, "Dynamic responses of a damaged double Euler – Bernoulli beam traversed by a ‘phantom’ vehicle, *Structural Control and Health Monitoring*, 1–31.